Final Technical Report

USGS-NEHRP Award Number #G11AP20002

Earthquake rupture dynamics: Factors controlling initial conditions and variability of rupture processes

Principal Investigator – James H. Dieterich
Department of Earth Sciences
University of California, Riverside
454 Geology Bldg
Riverside, CA 92521

Telephone 951-827-2976

Fax 951-827-4324,

E-Mail dieterichj@ucr.edu

Co-Principal Investigator – David D. Oglesby

Department of Earth Sciences
University of California, Riverside
454 Geology Bldg
Riverside, CA 92521

Telephone 951-827-2036

Fax 951-827-4324,

E-Mail david.oglesby@ucr.edu

Term covered by award – Dec 2010 – Nov 2011

ABSTRACT

Effective strategies to reduce earthquake losses depend in large measure on accurate quantitative predictions of earthquake ground motions in future earthquakes. Because ground motions are highly variable, and therefore uncertain, suites of synthetic seismograms that capture the likely range of motions in future earthquakes are needed for seismic resistance design of engineered structures. Earthquake rupture complexity is a strong determinant of ground motions, and current methods used to generate synthetic seismograms employ various improvised descriptions (of stress state or source motions) to represent rupture complexity and variability. Such descriptions no basis from direct observation of stresses and may correspond to physical states that are unlikely (or impossible) to realize in nature, which in turn may lead to systematic errors in estimation of ground motions. This project focuses on three related, but poorly understood, aspects of this problem: 1) The stress state at the initiation of rupture on faults with heterogeneous strengths and geometric complexities, 2) the complexity of earthquake ruptures, and 3) event-to-event variability of rupture processes. We employ physics-based simulations of long sequences of earthquakes (≥100,000 events M3.5-M7.1) to characterize evolution of stresses prior to large earthquake ruptures. Using the evolved stress states from the multi-event simulations to set initial conditions prior to large earthquakes, near-field ground motions are then computed with a fully dynamic finite element code. We find that simulations that employ evolved initial stress conditions have both qualitative and quantitative differences from simulations that use homogeneous or improvised descriptions of initial conditions. Compared to simulations with improvised conditions, the simulated earthquakes consistently have lower peak particle velocities (factors 0.2 – 0.6), exhibit greater variability in rupture style, and spontaneously develop features not reported in prior simulations. In particular, some events show great variability of rupture speed, including cases where rupture growth locally stalls for 1-10 seconds before resuming propagation.

.

Earthquake rupture dynamics: Factors controlling initial conditions and variability of rupture processes

Introduction

Because earthquake ground motions are highly variable, approaches for seismic resistance design of engineered structures are being developed that rely on suites of synthetic seismograms to capture the likely range of motions in future earthquakes. Simulations of earthquake ruptures are a central element of such calculations. Hence, to accurately portray the uncertain range of ground motions in future earthquakes, the uncertainty of parameters that control (or describe) rupture processes must be properly portrayed and evaluated. That includes characterization of local and regional heterogeneities that are more or less stationary over time, such as fault geometry, constitutive parameters, and elastic structure; and event-to-event variations arising from system dynamics. Of the dynamical heterogeneities, initial stress state relative to frictional strength is the principal control parameter of rupture processes [Day, 1982].

Rupture complexity and coherence are strong determinants of radiation patterns and amplitudes, and properly representing these aspects of the earthquake source represents a important challenge in predicting earthquake ground motions. Compared to the seismic wave fields generated by smooth coherent ruptures, complex ruptures (with heterogeneous stress drops, and varying rupture directions and speeds) result in less coherent waves fields, reduced extremes in peak ground motions, and attenuated directivity [Olsen and others, 2008]. Methods for generating synthetic seismograms based on deterministic rupture simulations currently incorporate rupture complexity through hypothetical characterizations of heterogeneous model parameters (*i.e.* initial stress state relative to fault friction parameters) [Guatteri *et al.*, 2003; Ripperger *et al.*, 2008; Olsen *et al.*, 2008], while kinematic approaches represent rupture complexity through stochastic descriptions of the fault motions [Hall *et al.*, 1995; Mai and Beroza, 2002; Hartzell, *et al.*, 2002; Guatteri*et al.*, 2004, Graves *et al.*, 2008; Frankel, 2009]. However, such improvised descriptions, However, such descriptions may correspond to physical states that are unlikely to be realized in nature, which may in turn lead to significant errors in estimation of ground motions. As illustrated below, improvised patterns of stress state in deterministic rupture simulations appear to systematically overestimate initial stress levels relative to frictional strengths, which results in more energetic and more coherent ruptures than might generally occur in nature.

In this project we investigate the factors that control complexity and variability of earthquake rupture dynamics and resulting ground motions. We focus on three related aspects of the problem: 1) The stress state at the initiation of rupture on faults with heterogeneous strengths and geometric complexities, 2) the complexity of earthquake ruptures, and 3) event-to-event variability of rupture processes.

Method of Analysis

To develop suites of initial stress conditions for simulations of earthquake rupture and near-source motions we employ the fast high-resolution, earthquake simulator RSQSim [Dieterich and Richards-Dinger, 2010]. This simulator is capable of generating long sequences of earthquakes

(up to $5x10^5$) in geometrically complex fault systems over a wide range of earthquake magnitudes. In these simulations, stress states on are determined by the dynamics of fault interactions, and continuously evolve through the occurrence of earthquakes across a range of magnitudes. Every large earthquake is preceded by numerous small earthquake events that create the stress conditions that permit earthquake ruptures to propagate over large distances in large events. In addition, earthquake nucleation with RSQSim arises spontaneously at a site determined by the system dynamics of stress evolution and rate-and state-dependent friction [Dieterich, 1992]. Hence, in addition to supplying initial stress states at the initiation of earthquake rupture, the RSQSim results also specify the nucleation site where dynamic ruptures initiate. Pairing of initial conditions with nucleation location may be very important – as shown by Oglesby [2005] under identical initial conditions, ruptures may propagate over long distances or quickly die depending on nucleation location.

Because RSQSim does not simulate the dynamic wave field, detailed simulations of rupture propagation and resulting near-field seismic are computed with fully dynamic 3D finite element rupture dynamics programs using the initial stress states and nucleation sites from the multi-event simulations. Most finite element results presented here were obtained with the program FaultMod, which was developed by Michael Barall (Invisible Software, inc.) [*Barall*, 2009]. Both RSQSim and FaultMod accept rate-state constitutive properties for fault slip and complex 3D fault geometries. Some initial results were obtained with the commercial finite element program DYNA3D.

In this phase of the study we employed models of a simple planar fault with a standard set of model parameters. Uncertainty relating to heterogeneous, but stationary, model parameters (constitutive parameters, fault geometry, normal stress) will be addressed in a subsequent study through repeated simulations with different characterizations of fault properties.

Dynamic Modeling with FaultMod

FaultMod is a 3D dynamic finite element code that uses a unique grid-doubling technique to allow finer discretization on the fault (where highest resolution is desired) than elsewhere in the model space. It allows for the modeling of spontaneous, dynamic earthquake rupture, slip, wave propagation, and ground motion. Fault geometry may be complex, and available frictional parameterizations include slip-weakening [*Palmer and Rice*, 1973; *Andrews*, 1976] and rate-and-state [*Dieterich*, 1979; *Ruina*, 1983]. FaultMod has been extensively tested through the Southern California Earthquake Center's (SCEC)/USGS Dynamic Earthquake Rupture Code Verification Exercise [*Harris et al*., 2009], and has been determined to be extremely accurate. FaultMod is parallelized for shared-memory machines; parallelization for distributed-memory systems is currently being implemented. It is numerically and memory efficient. Calculations involving over 2 million elements (100 m in size near the fault, 200 m elsewhere) for 1000 time steps to be computed in under 10 hours using slightly over 7 GB of memory and 8 processors. Simulations reported here were completed in 4 – 8 hours on a 7-node Macintosh XServe cluster. Because our goal is to compare the ground motion for different methods of assigning fault pre-stress, it is not crucial to calculate ground motion to extremely high frequency using low-velocity near-surface materials.

Multi-Event Modeling with RSQsim

RSQSim is a quasi-static boundary element code developed expressly for multi-earthquake simulations with complex fault systems. RSQSim incorporates simplifications and large-scale approximations based on analytic solutions to greatly reduce computation times [Dieterich, 1995; Dieterich and Richards-Dinger, 2010]. Simulation with RSQSim for this study typically consisted of ≥100,000 earthquakes M4<M<8).

The simulations employ the rate- and state-dependent formulation for sliding resistance [Dieterich, 1979, 1981; Ruina, 1983; Rice, 1983]

$$\tau = \sigma \left[\mu_0 + a \ln\left(\frac{\dot{\delta}}{\dot{\delta}*}\right) + b \ln\left(\frac{\theta}{\theta*}\right) \right] \qquad (1)$$

where μ_0 , a, and b are experimentally determined constants; $\dot{\delta}$ is sliding speed, θ is a state variable that evolves with time and slip and normal stress history; and $\dot{\delta}^*$ and θ^* are normalizing constants. The evolution of θ takes place over a characteristic sliding distance D_c and at steady-state $\theta_{ss} = D_c / \dot{\delta}$. In the simulations fault strength is fully coupled to normal stress changes through the coefficient of friction and through θ, which evolves with changes of normal stress as given by Linker and Dieterich [1992]. See Marone [1998] and Dieterich [2007] for detailed reviews of rate- and state-dependent friction and discussion of applications to earthquake processes.

Details of the RSQSim computational method are found in Dieterich and Richards-Dinger [2010]. An important aspect of this modeling approach is the use of event driven computational steps as opposed to time stepping at closely spaced intervals. The cycle of stress accumulation and earthquake slip at each fault segment is separated into three distinct phases designated as sliding states 0, 1, and 2. A fault element is at state 0 if stress is below the steady-state friction, as defined by rate- and state-dependent friction. In the model this condition is approximated as a fully locked element in which the fault strengthens as the frictional state-variable θ increases with time (*i.e.* $\theta = \theta_0 + t$) with modifications for normal stress changes. The transition to sliding state 1 occurs when the stress exceeds the steady-state friction. During state 1 conditions have not yet been met for unstable slip, but the fault progressively weakens as frictional state evolves. Macroscopic slip is negligible. The nucleation solutions of Dieterich [1992] modified to take into account normal stress changes together with stressing rate determine the event transition time to state 2, which is earthquake slip. In Dieterich [1995] slip speed during an earthquake was set at a constant value using the relationship for elastic shear impedance together with the local dynamic driving stress

$$\dot{\delta}_{EQ_j} = \frac{2\beta\Delta\tau_j}{G} \ , \qquad (2)$$

where $\Delta\tau_j$ is the difference between the stress at the initiation of slip and the sliding friction at node j, b is the shear wave speed, and G is the shear modulus. The use of (2) provides a quasi-dynamical basis for introducing time into the earthquake event simulations and for setting slip speeds during an earthquake. An element ceases to slip and reverts to state 0 when the stress decreases to some specified stress determined by the sliding friction (stress overshoot and randomization of final stress at end of slip are optionally permitted). This approach avoids computationally intensive solutions of systems of equations at closely spaced time intervals.

Computation time for an event of some fixed size embedded in a model with n fault elements scales by $n^{\sim 1}$.

Results

Modeling efforts with RSQSim focused primarily on idealized faults to better understand the characteristics of stress interactions that control earthquake statistics, and to test the simulation code. Initial simulations were obtained with simple models of planar faults with a consistent set of model parameters – nominal normal stress of 120 MPa (except for prescribed patches with normal stresses from 125Mpa to 150MPa) initial shear stress of 100 MPa and rate state parameters of m=0.57, a=0.01 and b=0.0168.

Earthquakes rupture growth can be crack-like or consist of a narrow slip-pulse (Heaton, 1990). With RSQSim factors favoring crack-like behavior are relatively smooth initial stresses, weak healing (re-strengthening of the fault) following termination of slip, and unconstrained rupture growth; while slip-pulse behavior arises with heterogeneous initial stresses and strong fault healing following rupture termination (Figure 1). This behavior is consistent with fully dynamical rupture simulations [Beroza and Mikumo, 1996; Zheng and Rice, 1998]. With RSQSim healing is controlled by the rate-state frictional parameters and by a dynamic stress overshoot parameter that determines the shear stress at the termination of slip relative to the sliding friction. During an earthquake, if sliding stops at stresses that are sufficiently below the sliding friction, then healing outpaces re-stressing from continuing slip on adjacent regions of the fault. This inhibits renewed or continuing slip and leads to pulse-like ruptures. Conversely, if sliding stops at or only slightly below the sliding friction, then continuing slip on adjacent regions of the fault can immediately trigger renewed sliding before healing can occur. This effect favors on- and off switching of slip, which approximates continuous slip over broad regions at slower slip speeds, which is characteristic of crack-like ruptures. In the simulations reported here, the overshoot factor was adjusted to give results that best reproduce the finite element rupture simulations.

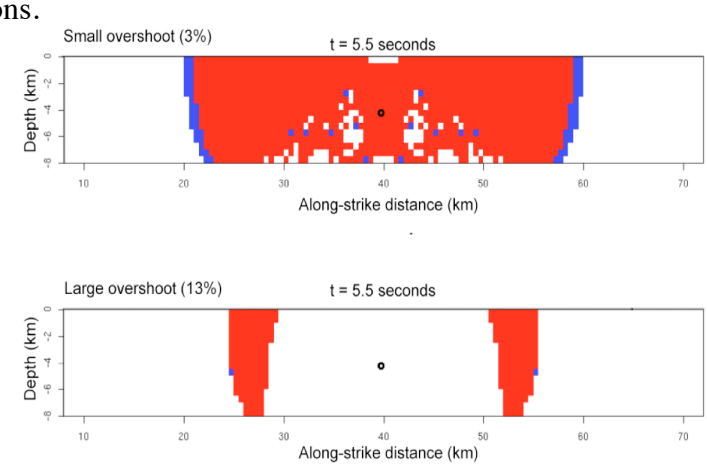

Figure 1*. Snapshots of actively slipping regions (red), 5.5 seconds after start of a bilateral earthquake rupture on a strike-slip fault, showing crack-like rupture growth (upper frame) and slip pulse behavior (lower frame). Blue areas are at sliding state 1 (nucleation) and white regions are at state 0 (locked). Both simulations use identical model parameters except for the stress overshoot factor, which specifies stress relative to sliding friction at the termination of slip. Note slower rupture propagation in pulse-like ruptures.*

Although RSQSim employs approximations of the earthquake rupture processes to achieve computational efficiency (seismic wave propagation is not modeled) we believe those approximations do not seriously distort the results for modeling stress evolution and stress states at the onset of earthquake rupture events, which are subjects of this study. Key performance measures for modeling stress evolution leading to large earthquakes are the accuracies with which the calculations represent a) nucleation processes that determine the time and place of initiation of earthquake slip events, b) the spatial extent of earthquake rupture given a stress state at the initiation of the event, and c) the slip distribution in that event, which determines the details of the stress state following the event (and therefore the subsequent history). The analytic nucleation solutions used in RSQSim have been shown to be effective in predicting the evolution of slip speed during nucleation and hence nucleation times as observed in laboratory experiments [Dieterich and Kilgore, 1996] and in detailed models with rate-state friction [Dieterich, 1992; Fang and others, 2010]. To test items b) and c) we have undertaken a program of tests that compare single-event RSQSim earthquake simulations with detailed fully dynamic finite element calculations.

Figure 2 compares a simulation with RSQSim and a fully dynamic 3D finite element rupture simulation. In this example the finite element code used was DYNA3D. This example is for a planar strike-slip fault that extends to the free surface, with idealized asperities consisting of eight patches with higher normal stress relative to the background normal stress of 120 MPa. In this simulation a uniform initial shear stress is set just above the minimum value that results in rupture propagation across the entire fault surface for forced nucleation near the left end of the model (indicated by the **+** symbol). While some details of rupture propagation with RSQSim differ from results obtained with DYNA3D, the simulations are quite similar in most respects, including rupture complexity. The RSQSim computation time is about 10^{-3} of that required by DYNA3D. Because of the computation time scaling by $\sim n^{1}$ RSQSim that computational advantage rapidly increases as system size increases.

Several multi-event simulations, consisting of 200,000 earthquakes have been carried out to survey the effects stress evolution and fault patch heterogeneities on rupture processes. Most earthquakes are small, but typically there are 50-125 end-to-end M≥7 events in each simulation. Figure 3 illustrates some effects of stress evolution on large-event rupture propagation from one set of simulations. The first earthquake in this simulation is the event illustrated in Figure 2, which initiates from the initial prescribed uniform stress state. Note that subsequent large events differ both qualitatively and quantitatively from the initial rupture. In particular the later events with evolved stress states 1) have longer rupture durations with lower average rupture speeds; 2) have lower stress drops; 3) show no evidence of the stronger patches (areas of higher normal stress) in either the total slip or rupture propagation and 4) have considerable event-to-event variability in the characteristics of rupture propagation, including smoothly propagating ruptures and event in which rupture propagation momentarily halt and for intervals of 1 to 5 seconds;

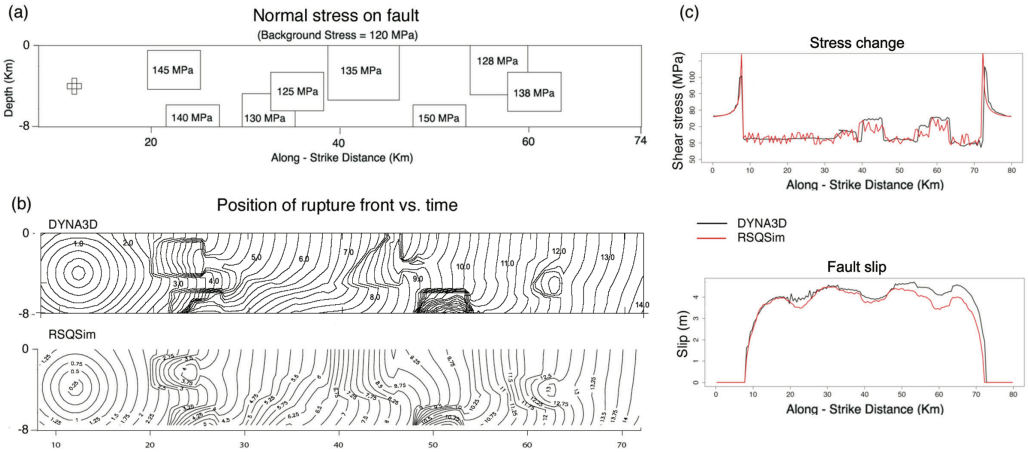

Figure 2. *Comparison of rupture simulations using the fast simulator RSQSim and the detailed and fully dynamic finite element model DYNA3D. (a) Normal stress distribution on fault surface. (b) Rupture initiation time (the contours map the rupture front as a function of time). (c) Final stress (upper panel) and slip (lower panel) along a profile at depth of 4.25 km. Fault elements for this simulation are 500 m x 500 m. Times for ruptures to reach the end of model differ by about 2%.*

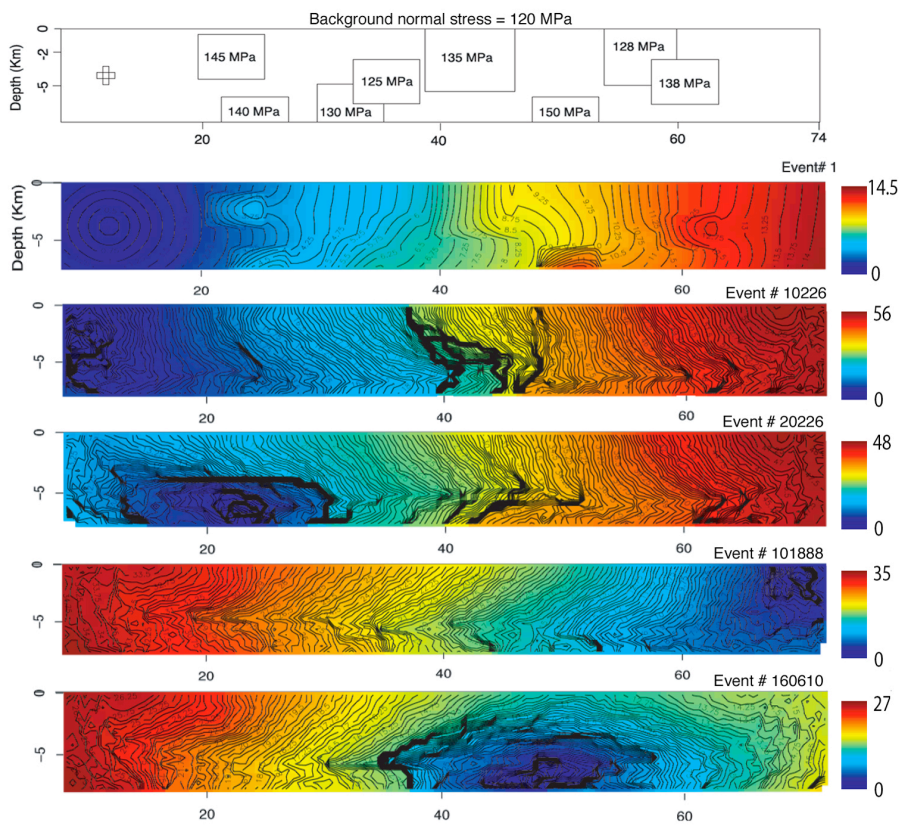

Figure 3. *Rupture initiation time for large earthquakes from a multi-event simulation with 200,000 earthquakes ~M3.5-M7.1. The contours and color indicate the progression of the rupture front with time. The uppermost color panel (event 1) is the first earthquake (also shown in Figure 2) that initiated with uniform initial shear stress. The lower panels show a sample of later large end-to-end ruptures that initiated from evolved stress states during the simulation. Bunching of contours (black regions) reflect temporary halts of rupture propagation lasting from 1-5 seconds. Note that the high strength regions have no observable effect on rupture propagation in the later events.*

Examples of dynamic rupture simulations with FaultMod are shown in Figures 4 and 5. The examples Figure 4 illustrate characteristics of simulations with uniform conditions (4a) and models of composed initial (stress/strength) conditions (4b). Figure 4a illustrates a rupture with uniform normal stresses of 120MPa, and uniform initial shear stress of 100 MPa. The upper panel shows the position of the rupture front as a function of time and the lower panel gives peak horizontal particle velocity at the free surface. The example in 4b is for a model similar to that in Figure 2, with arbitrarily placed stronger patches having normal stresses in the range 125Mpa to 150MPa, compared to normal stress of 120 on the remainder of the fault. As in 4a the initial shear stress is 100MPa. Peak particle motions are 2.0m/s and 1.7m/s in 4a and 4b, respectively. The rupture propagation speeds in 4a increase with distance from the nucleation zone reaching ~ 5km/s, while propagation speeds in 4b are variable but have average values of ~2.7 km/s away from the nucleation zone. Note the strong directivity in each model with indications of incoherence as rupture encounters the strong patches in 4b.

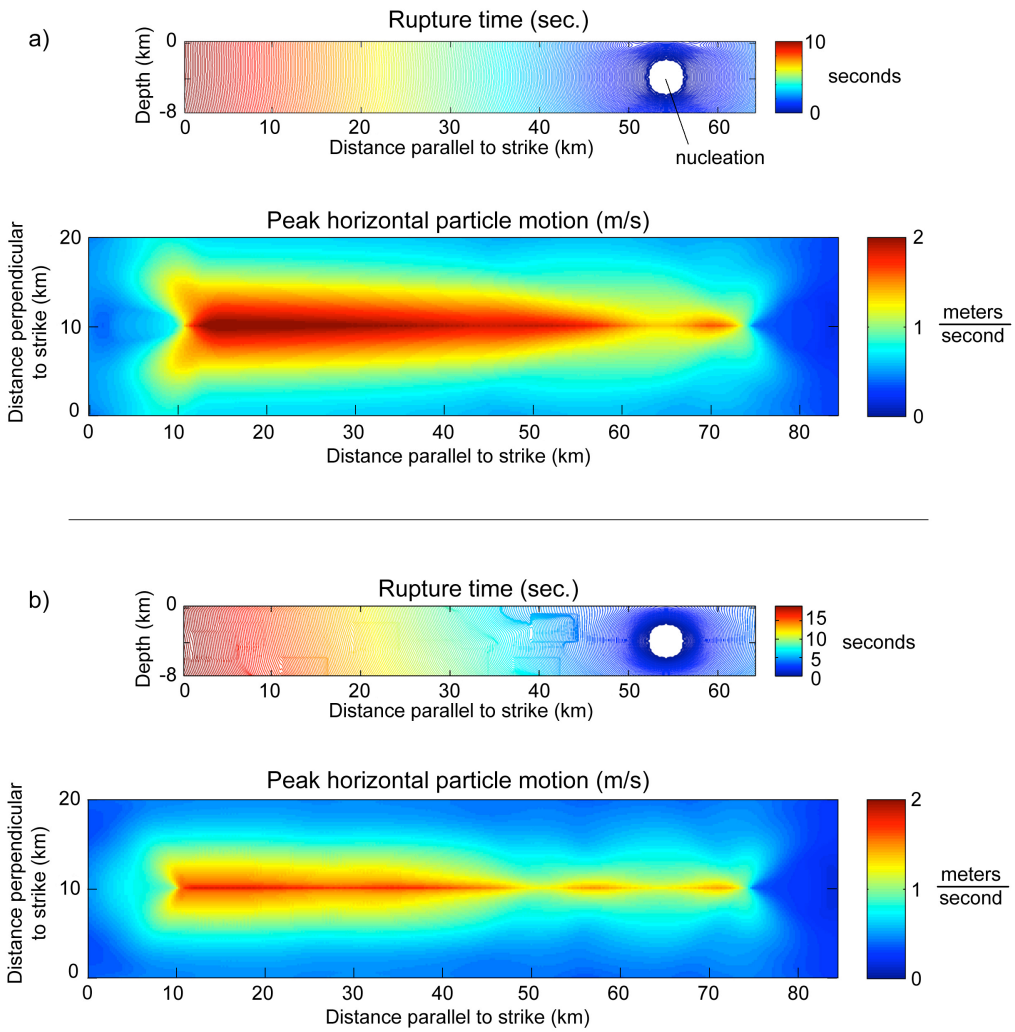

Figure 4. Rupture propagation and peak particle motions in simulations with uniform initial shear stress of 100MPa computed with the finite element code FaultMod. These examples are of a planar strike-slip fault that extends to the free surface. The white circular patch marks the location of forced nucleation. a) Model with uniform normal stress of 120 MPa. b) Model with uniform background normal stress of 120 MPa, together with stronger patches of elevated normal stress (125-150MPa).

The two examples in Figure 5 employ the model with stronger patches (as in Figure 4b) and use initial stresses prior to end-to-end ruptures from the multi-event RSQsim simulations. The location of the forced nucleation in these examples corresponds to the location of the spontaneous nucleation in the multi-event simulations. The example in 5a illustrates, start-stop-start rupture propagation effects observed for many RSQSIm events (Figure 3). In this case rupture propagation paused for about 10 seconds shortly after nucleation. Prior to the pause rupture propagation speeds were ~ 0.5km/s and after the pause, rupture propagation speeds quickly increased to ~ 2.5km/s. Peak particle motions in 5a are about 0.85 m/s. In the example of 5b a bilateral rupture immediately propagates to the left with delayed onset of rupture to right. Initial propagation speeds are roughly 1km/s increasing to about 2.7km/s. Peak particle motion is 1.15m/s.

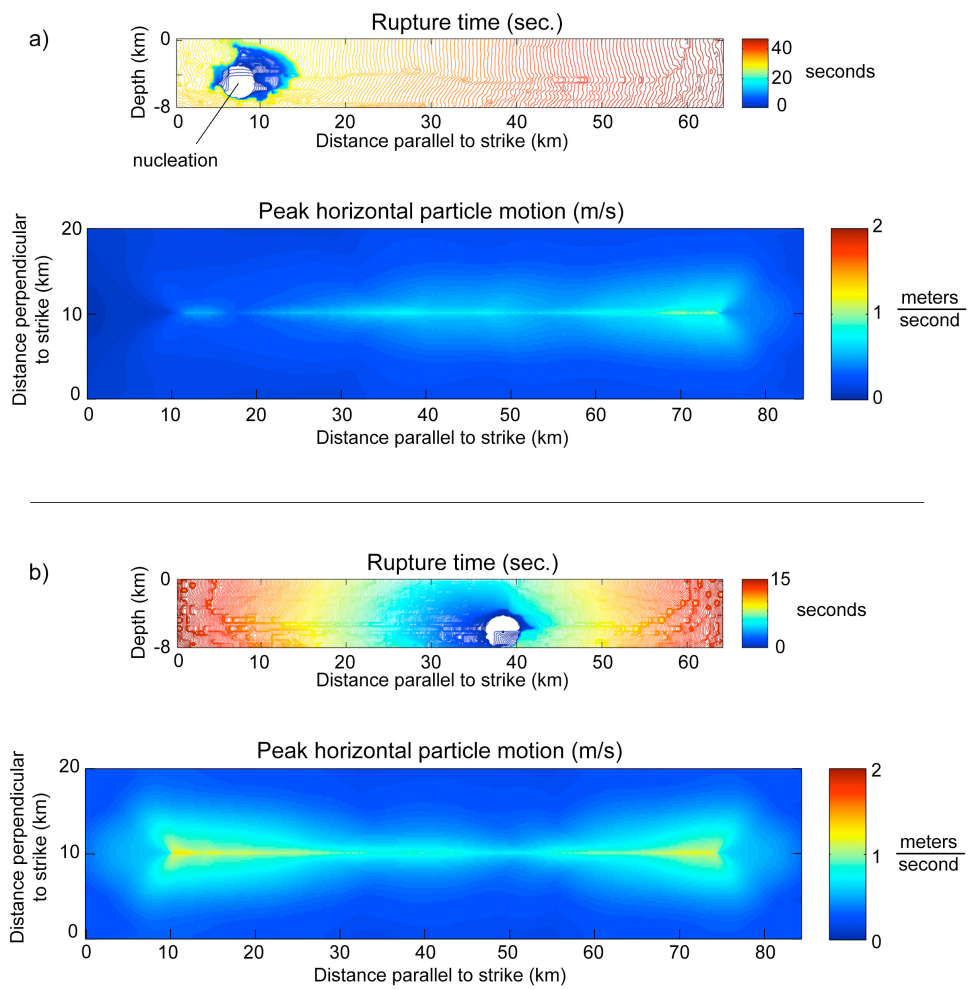

Figure 5. Examples of rupture propagation and peak particle motions in simulations with evolved initial stress states imported from the multi-event RSQSim simulations. These examples are of a planar strike-slip fault that extends to the free surface. The model has uniform background normal stress of 120 MPa, with stronger patches of elevated normal stress (125-150MPa) as in the example of Figure 4b. The white circular patch marks the location of forced nucleation. a) Model with uniform normal stress of 120 MPa. b) Model with uniform background normal stress of 120 MPa, together with stronger patches of elevated normal stress (125-150MPa).

Discussion and Conclusions

Although full analysis the extensive data sets generated by these simulations remains to be carried out, the preliminary results presented here point to a number of interpretations and conclusions that are broadly relevant to simulations of earthquake ground motions.

Comparisons with fully dynamic finite element models of earthquake rupture and slip demonstrate that the RSQSim multi-event simulations represent, with accuracy, the process of stress evolution in fault systems wherein the system dynamics of fault interactions that determine the initial stress conditions (relative to fault strength) for subsequent earthquakes. Because earthquake rupture and ground motion models are very sensitive to initial conditions the use of evolved initial conditions from simulations can provide significant improvements in 1) earthquake rupture and ground motion models and 2) evaluation of uncertainties arising from event-to-event variations of rupture processes. In contrast to this, current methods to specify heterogeneous initial conditions employ largely *ad hoc* assumptions of heterogeneity and may result in physical states (stress relative to strength) that cannot be reached by natural systems. Also the approach investigated in this study enables evaluation uncertainties in ground motions arising from uncertain model parameters. For a fixed set of initial conditions, simulations of earthquake rupture and ground motions depend on uncertain model parameters, such as constitutive properties and fault geometry. Because these parameters also affect simulations of stress evolution, model uncertainties can be propagated through the multi-event simulation and ground motion models in comprehensive and consistent fashion. Finally, it appears feasible to also use the RSQSim simulator technology to generate physics-based descriptions earthquake sources for use as kinematic inputs for generation of synthetic of synthetic seismograms, which are computationally more efficient than methods that directly employ deterministic rupture simulations.

Significantly, we find that rupture simulations using evolved initial stress conditions differ both quantitatively and qualitatively from simulations with uniform initial conditions or improvised models with composed stress or strength heterogeneity. Compared to simulations with improvised conditions, simulated earthquakes consistently have lower peak particle velocities (by factors of 0.2 to 0.6), longer durations for a given earthquake magnitude, and greater variability in rupture style. In addition we consistently obtain smaller stress drops for events with evolved initial stresses. For example, in the simulation of Figure 3 the uniform initial stress for the first rupture was set, by trial-and-error to be slightly above the minimum uniform shear stress needed to fully rupture the entire fault for the specified point of nucleation. The stress drop of that first event was 10.6 MPa compared to a mean value of 5.6 MPa for the later M≥7 events. Perhaps the most striking feature of these simulations is the local variability of rupture speeds wherein rupture growth temporarily halts for intervals of up to 10 seconds before resuming propagation (Figures 3 and 5). This start-stop-start characteristic results in less coherent radiation and appears to be at least partly responsible for the longer event durations and lower peak particle speeds.

We believe these differences arise because the process of stress evolution that condition faults to fail in large earthquakes is not a purely random process that can be readily reproduced by *a priori* models of initial conditions. In the multi-event simulations, and presumably in nature, small earthquakes occurring at different locations play an important role in transferring stress to

areas that halted rupture growth due to low stress, relative to the local strength. In addition the small events, which can be viewed as failed large earthquakes, frequently test the system to optimal locations for nucleation under minimal stress conditions. The resulting ruptures with evolved initial stresses often have locally sluggish start-stop-start propagation, and are less coherent with lower peak particle velocities than simulations with improvised representations of strength heterogeneity.

Publications

In preparation

References

Aki, K., and P. G. Richards, 2002, Quantitative Seismology, 2nd Ed., University Science Books.

Andrews, D.J., Rupture propagation with finite stress in antiplane strain, *Journal of Geophysical Research*, *81* (20), 3575-3582, 1976.

Barall, M., A grid-doubling technique for calculating dynamic three-dimensional spontaneous rupture on an earthquake fault, *Geophysical Journal International*, *178*, 845-859, 2009.

Day, S. M., 1982, Three-dimensional simulation of spontaneous rupture: theeffect of nonuniform prestress, *Bull. Seism. Soc. Am.* **72,** 1881–1902.

Dieterich, J. H., 1979, Modeling of rock friction 1. Experimental results and constitutive equations, J. Geophys. Res., 84, 2161–2168.

Dieterich, J., 1981, Constitutive properties of faults with simulated gouge, in Monograph 24, Mechanical Behavior of Crustal Rocks, edited by N. L. Carter, M. Friedman, J. M. Logan, and D. W. Sterns, pp. 103–120, American Geophysical Union, Washington, D.C..

Dieterich, J.H., 1995, Earthquake Simulations with Time-Dependent Nucleation and Long-Range Interactions, *Journal of Nonlinear Processes in Geophysics* , 2, 109-120.

Dieterich, J.H., 1992, Earthquake nucleation on faults with rate- and state-dependent friction, *Tectonophysics, 211*, 115-134.

Dieterich, J., 2007, Applications of rate-and-state-dependent friction to models of fault slip and earthquake occurrence, in Treatise On Geophysics, Vol. 4, edited by G. Schubert, Elsevier, Oxford.

Dieterich J. H., Kilgore B. Implications of Fault Constitutive Properties for Earthquake Prediction. Proceedings of the National Academy of Science 93:3787–3794, 1996.

Dieterich, J. H., and K. Richards-Dinger, Earthquake recurrence in simulated fault systems, Pure Appl. Geophys., doi:10.1007/s00024-010-0094-0, 2010.

Guatteri, M., Mai, P. M., Beroza, G. C., and J. Boatwright, 2003, Strong Ground-Motion Prediction from Stochastic-Dynamic Source Models, *Bull. Seism. Soc. Am.*, **93**, 301-313; DOI: 10.1785/0120020006

Graves, R. W., Aagaard, B., Hudnut, K., Star, L., Stewart, J., and Jordan, T. H. , 2008, Broadband simulations for Mw 7.8 southern San Andreas earthquakes: Ground motion sensitivity to rupture speed, *Geophys. Res. Lett.*, **35**, L22302, doi:10.1029/2008GL035750.

Fang, Z., J. H. Dieterich, and G. Xu, Effect of initial conditions and loading path on earthquake nucleation, J. Geophys. Res., 115, doi:10.1029/2009JB006558, in press.

Hall, J., Heaton, T., Halling, M., and Wald, D., 1995, Near-source ground motion and its effects on flexible buildings, *Earthquake Spectra* **11,** 569–605.

Harris, R.A., M. Barall, R.J. Archuleta, E.M. Dunham, B. Aagaard, J.-P. Ampuero, H.S. Bhat, V. Cruz-Atienza, L. Dalguer, P. Dawson, S.M. Day, B. Duan, G. Ely, Y. Kaneko, Y. Kase, N. Lapusta, Y. Liu, S. Ma, D.D. Oglesby, K.B. Olsen, A. Pitarka, S.G. Song, and E. Templeton, The SCEC/USGS dynamic earthquake rupture code verification exercise, *Seismological Research Letters*, *80* (1), 119-126, 2009.

Hartzell, S., Leeds, A., Frankel, A., Williams, R., Odum, J., Stephenson, W., and Silva, W., 2002, Simulation of broadband ground motion including nonlinear soil effects for a magnitude 6.5 earthquake on the Seattle fault, Seattle, Washington, *Bull. Seism. Soc. Am.* **92,** 831–853.

Linker, M. F., and J. H. Dieterich, 1992, Effects of variable normal stress on rock friction - Observations and constitutive equations, J. Geophys. Res., 97, 4923–4940.

Mai, P. M., and G. C. Beroza, 2002, A spatial random field model to characterize complexity in earthquake slip, J. Geophys. Res., 107(B11), 2308, doi:10.1029/2001JB000588.

Meade, B. J., 2007, Algorithms for the calculation of exact displacements, strains, and stresses for triangular dislocation elements in a uniform elastic half space, *Computers & Geosciences,* **33**, 1064-1075.

Marone C (1998) Laboratory-Derived Friction Laws and Their Application to Seismic Faulting. *Annual Review of Earth and Planetary Sciences* **26**, 643–696, DOI 10.1146/annurev.earth.26.1.643

Oglesby, D.D., 2005, The Dynamics of Strike-Slip Step-Overs with Linking Dip-Slip Fualts, *Bull. Seism. Soc. Am.* **95,** 1604-1622.

Okada Y., 1992, Internal deformation due to shear and tensile faults in a half-space, *Bull Seismol Soc Am*, **82**:1018–1040

Olsen, K. B., Day, S. M., Minster, J. B., Cui, Y., Chourasia, A., Okaya, D., Maechling, P., and Jordan,T., 2008, TeraShake2: Spontaneous Rupture Simulations of M_w 7.7 Earthquakes on the Southern San Andreas Fault, *Bull. Seism. Soc. Am.*, **98**; 1162-1185; DOI: 10.1785/0120070148

Palmer, A.C., and J.R. Rice, The growth of slip surfaces in the progressive failure of overconsolidated clay, *Proceedings of the Royal Society of London*, *A332*, 527-548, 1973.

Rice, J. R., 1983, Constitutive relations for fault slip and earthquake instabilities, Pure and Applied Geophysics, 121, 443–475.

Ripperger, J., Mai, P. M., and Ampuero,J.-P., 2008, Variability of Near-Field Ground Motion from Dynamic Earthquake Rupture Simulations, *Bull. Seism. Soc. Am.*, **98**, 1207-1228; DOI: 10.1785/0120070076

Ruina, A., 1983, Slip instability and state variable friction laws, J. Geophys. Res., 88, 10,359–10,370.

Zheng, G., and Rice, J. R., 1998, Conditions under which velocity-weakening friction allows a self-healing versus a crack-like mode of rupture, Bull. Seismol. Soc. Am., 86 , 1466–1483.